Optik - International Journal for Light and Electron Optics 216 (2020) 164856

Contents lists available at ScienceDirect

Optik

journal homepage: www.elsevier.com/locate/ijleo

Original research article

Accurate Closed Form Expressions for The Time-Bandwidth Product and FCC Violation Ratio as New Metrics To Characterize UWB Optical Systems

Eslam A. Aly[a], Mostafa B. Alabd[a], Nouran Kassem[a], Waleed Mustafa[c], Mohamed Shehata[a], Hassan Mostafa[a,b,*]

[a] Electronics and Communications Engineering Department, Cairo University, Giza 12613, Egypt
[b] University of Science and technology, Nanotechnology and Nanoelectronics Program, Zewail City of Science and Technology, October Gardens, 6th of October, Giza 12578, Egypt
[c] Communications and Information Engineering Department at Zewail City for Science and Technology, Cairo, Egypt

ARTICLE INFO

Keywords:
UWB
TBP
FCC
Gaussian Pulse
Sech Pulse

ABSTRACT

In this paper, analytical analysis of the first seven derivatives of the Gaussian and hyperbolic secant pulses is carried out for a basic optical communications system. The analysis is mainly based on two important design metrics, namely the Federal Communications Commission violation ratio (FCC VR), and the time-bandwidth product (TBP). The FCC VR is a new metric introduced in this paper, it computes the average power of the signal violating the FCC mask relative to the average power of the FCC mask over the whole spectrum. FCC VR provides great insight on how a generated UWB pulse obeys the FCC mask. The second metric discussed in this paper is the TBP, which is obtained using a variance-based definition for the pulse width. This definition is advantageous in many aspects compared to other definitions, as discussed in the paper. In this work, a generalized closed-form expressions is obtained for the TBP regarding the aforementioned pulse shapes. Moreover, the analysis of a basic optical communications system is carried out by applying the two metrics which proves their significance in the context of designing a similar system.

1. Introduction

Wirelessand RF services have become a necessity in modern daily life, new technologies and advances are continuously emerging in this field. However, great advances always meet limitations. The congestion of the radio spectrum by the current RF services is one of the most challenging limitations. It became harder for new technologies and services to fit in the spectrum without interfering with existing services. Therefore, the Federal Communications Commission (FCC) regulates the spectrum among all existing and new RF services. Moreover, the congestion problem continues to be a major issue due to the ever-increasing number of users demanding access to a wide range of information as fast and secure as possible, anytime and anywhere [1][2].

Thus, a proposed idea, introduced mainly for the short-range communications, was the Ultra-Wide Band *(UWB)*; which is a technology that is based on the spread of the radio energy over a very wide range of frequency band, with a very low-power spectral

* corresponding author.
E-mail addresses: Es.Atef@outlook.com (E.A. Aly), mostafaabahaa@yahoo.com (M.B. Alabd), nourankassem97@gmail.com (N. Kassem), s-wmustafa@zewailcity.edu.eg (W. Mustafa), hmostafa@uwaterloo.ca (H. Mostafa).

https://doi.org/10.1016/j.ijleo.2020.164856
Received 1 February 2020; Received in revised form 13 April 2020; Accepted 29 April 2020

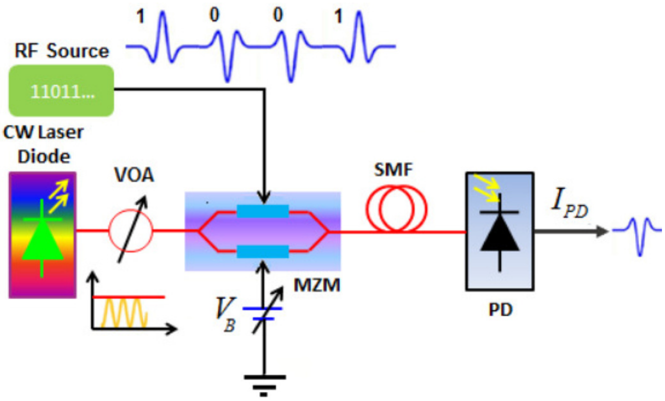

Fig. 1. Basic Optical system diagram [3].

density; having the maximum PSD as -41.3 dBm in the range of 3.1 GHz to 10.6 GHz, that is known as the useful ultra-wide band. The low power spectral density limits the interference with the traditional RF services occupying the spectrum, and the large bandwidth allows for a very high data rate for the communications system[3]. In this paper, an analytic analysis of the first seven derivatives of the Gaussian and the hyperbolic secant pulses is carried out through a fundamental optical communications system, shown in Fig. 1. This analysis is based on two important metrics; the time-bandwidth product *(TBP)*, and the FCC Violation ratio ratio *(FCC VR)*, which is introduced in this work.

The paper is organized as follows; in section II, the system components and their role are discussed. In section III, the TBP is introduced and mathematically derived for the m^{th}-order derivative of the Gaussian and Sech pulses. In section IV, the FCC VR is also introduced and mathematically formulated. In section V, a general optical communications system is analyzed by applying the TBP and the FCC VR as design metrics, characterizing the design trade-offs present in a similar system.

2. System Overview

The system in in Fig. 1 consists of continuous wave (CW) laser diode (LD), followed by variable optical attenuator (VOA), which controls the optical power of laser diode output signal. Then, the Mach-Zhender modulator which is an electro-optic modulator used for amplitude modulation of optical signals. Finally, the amplified signal passes through the optical standard single-mode fiber (SMF) followed by the photo-detector, which is used to convert the received optical signal to electrical signal[3].

3. Time-Bandwidth product

The time-bandwidth product (TBP) is defined as the product of the temporal width and the spectral width of a pulse. In ultra-fast laser physics, it is common to define the width of a pulse as the full width at half-maximum *(FWHM)* in both time- and frequency-domain. However, in this paper, a different definition of the pulse width is applied for reasons to be discussed later in the section.

Transform-limited pulses (as opposed to chirped-pulses) have the minimum possible TBP. Therefore, TBP is often used for indicating how close a pulse is to the transform limit, by indicating how close the pulse duration is to the limit which is set by its spectral width.

3.1. The mathematical definition

The normalized nth moment functions in both time and frequency domains are first established, for a pulse described by $\Psi(X)$, as follows:

$$\langle X^n \rangle = \frac{\int_{-\infty}^{\infty} X^n\ |\Psi(X)|^2 dt}{\int_{-\infty}^{\infty} |\Psi(X)|^2 dX} \tag{1}$$

Where X is set as t to donate time domain, and ω to donate frequency domain.

Furthermore, the temporal and spectral widths are defined based on the definition of the standard deviation as follows:

$$\Delta t = \sqrt{\langle t^2 \rangle - \langle t \rangle^2} \tag{2}$$

$$\Delta\omega = \sqrt{\langle \omega^2 \rangle - \langle \omega \rangle^2} \tag{3}$$

Thus, the TBP is defined in the following form:

$$\text{TBP} = \Delta\omega.\ \Delta t \tag{4}$$

The previous definition of the temporal width and the spectral width in (2) and (3) respectively has some advantages over the definition of the FWHM. Most importantly: its highly invariant mathematical definition that depends only on the pulse shape. Such a definition accurately characterizes odd functions such as the first derivative of the Gaussian pulse, unlike the FWHM. This proves very useful in the analysis carried out in this paper. In subsections B and C, the TBP for the Gaussian and hyperbolic secant pulses of general order derivatives are analytically derived. To analytically define the TBP of a pulse, the integrals from (1) (time- and frequency-domain moment functions) must be evaluated first.

3.2. The Gaussian pulse

Both temporal- and spectral-width derivations for the Gaussian pulse will be established in the following subsections to obtain a closed form for the TBP of the mth-order derivative of the Gaussian pulse.

3.2.1. The frequency domain

The following integral is to be evaluated to determine the spectral-width of the Gaussian pulse of general mth-order derivative:

$$\mathrm{I} = \int_{-\infty}^{\infty} \omega^n |G^{(m)}(\omega)|^2 d\omega \tag{5}$$

Where the input basis function is the amplitude of the normalized Gaussian pulse, substituting in (5) leads to:

$$\mathrm{I} = \int_{-\infty}^{\infty} \omega^{n+2m} e^{-\frac{\tau^2}{2}\omega^2} d\omega \tag{6}$$

This integral can be analytically evaluated to a closed formula through applying the repetitive differentiation of the Gaussian integral, which leads to (6) being analytically evaluated as the following expression:

$$\mathrm{I} = \begin{cases} \dfrac{(2m+n-1)!\sqrt{\pi}}{2^{m+0.5n-1.5}\left(\frac{n+2m-2}{2}\right)!\tau^{2m+n-1}} & ,\ \text{evenn},\ \mathrm{n} \neq 0,\ 2\mathrm{m}+\mathrm{n} \neq 0 \\ \sqrt{\dfrac{2\pi}{\tau^2}} & ,\ 2m+n=0 \\ 0 & ,\ \text{otherwise} \end{cases} \tag{7}$$

3.2.2. The time domain

Similarly, the following integral is to be evaluated to determine the temporal-width of the Gaussian pulse of general mth-order derivative:

$$\mathrm{I} = \int_{-\infty}^{\infty} t^n |g^{(m)}(t)|^2 \mathrm{dt} \tag{8}$$

By substituting for the time domain expression for the Gaussian pulse, (8) leads to:

$$\mathrm{I} = \int_{-\infty}^{\infty} t^n \left(-\frac{1}{\tau}\right)^{2m} e^{-2\left(\frac{t}{\tau}\right)^2} H_m^{\left(\frac{t}{\tau}\right)^2} \mathrm{dt} \tag{9}$$

Where H_m is the Hermite Polynomial of order m.

It is seen that squaring and multiplying the Hermite polynomial by $t^n e^{-2t^2}$ would result in the sum of integrals similar to that of the frequency domain case (6), so (9) will be analytically evaluated as follows:

$$I = \tau^{n+1-2m}(m!)^2\sqrt{\pi}\left[\begin{array}{l} z(n,m) + \displaystyle\sum_{j=0}^{\left\lfloor\frac{m}{2}\right\rfloor-1} \frac{2^{-(m-2j+1.5n-0.5)}(2m-4j+n-1)!}{(j!)^2(m-2j)!^2(m-2j+\frac{n}{2}-1)!} + \\ \displaystyle\sum_{j=0}^{\left\lfloor\frac{m}{2}\right\rfloor}\sum_{i=0}^{j-1} \frac{(-1)^{i+j}2^{-(m-i-j+1.5n-1.5)}(2m-2(i+j)+n-1)!}{j!i!(m-2j)!(m-2i)!(m-(i+j)+0.5n-1)!} \end{array}\right] \tag{10}$$

Where $z(n, m)$ is given by:

$$z(n,m) = \begin{cases} \dfrac{(n+1)2^{-1.5n+0.5}(n-1)!}{\left(\left(\left\lfloor\frac{m}{2}\right\rfloor\right)!\right)^2(0.5n-1)!} & ,\text{niseven andmisodd} \\ \dfrac{2^{-1.5n+0.5}(n-1)!}{\left(\left(\left\lfloor\frac{m}{2}\right\rfloor\right)!\right)^2(0.5n-1)!} & ,\text{niseven andmiseven} \\ \dfrac{1}{\left(\left(\left\lfloor\frac{m}{2}\right\rfloor\right)!\right)^2\sqrt{2}} & ,\ n=0 \end{cases} \tag{11}$$

By substituting for n and m in the equations from (7), (10), and (11); analytically determining the TBP for a general m$^{\text{th}}$-order derivative Gaussian pulse is feasible.

3.3. The hyperbolic secant pulse

Both temporal- and spectral-width derivations for the hyperbolic secant pulse will be established in the following subsections to obtain a closed form for the TBP of the m$^{\text{th}}$-order derivative of the hyperbolic secant pulse.

3.3.1. The frequency domain

The following integral is to be evaluated to determine the spectral-width of the hyperbolic secant pulse of general m$^{\text{th}}$-order derivative:

$$\mathrm{I} = \int_{-\infty}^{\infty} \omega^n |S^{(m)}(\omega)|^2 d\omega \tag{12}$$

The previous equation is then analytically evaluated as follows [4]:

$$I = \frac{2}{\pi}\left(\frac{2}{\tau}\right)^{n+2m+1} B_{n+2m}\left(\frac{1}{2}\right) \tag{13}$$

Where $B_i(x_0)$ is the Bernoulli polynomial of order i substituted in with point x_0.

3.3.2. The time domain

Similarly, the following integral is to be evaluated to determine the temporal-width of the hyperbolic secant pulse of general m$^{\text{th}}$-order derivative

$$\mathrm{I} = \int_{-\infty}^{\infty} t^n |s^{(m)}(t)|^2 \mathrm{d}t \tag{14}$$

The previous equation is analytically evaluated in the following form:

$$I = \sum_{r=0}^{\lfloor \frac{m}{2} \rfloor} (E_m^r)^2 \sum_{k=0}^{m-2r} \binom{m-2r}{k} A_k + 2\sum_{r=0}^{\lfloor \frac{m}{2} \rfloor} \sum_{j=0}^{r-1} E_m^r E_m^j \left[\sum_{k=0}^{m-2r} (-1)^{r+j} \binom{m-r-j}{k} A_k \right] \tag{15}$$

Where A_k is defined as:

$$A_k = (-1)^k \int_{-\infty}^{\infty} \mathrm{sech}(t)^{2k+2} t^n \mathrm{d}t \tag{16}$$

And where E_a^b is the double-indexed Euler number, defined for constants a and b. The double-indexed Euler number is defined recursively by the following equation:

$$E_m^r = E_{m-1}^{r-1}(m-2r+1) + E_{m-1}^r(n-2m) \,\text{and}\, E_m^0 = m! \tag{17}$$

The integral in (16) is then evaluated in Table 1 by taking the limits to the expression in (18) from [5].

$$\begin{aligned} \left(\int x^k \mathrm{sech}^n(x)\mathrm{d}x\right) &= -2^n e^{-\mathrm{nx}}\Big[\frac{x^k}{n}\,{}_2F_1\Big(n, \frac{n}{2}; \frac{n+2}{2}; -e^{-2x}\Big) \\ &+ \frac{\mathrm{kx}^{k-1}}{n^2}\,{}_3F_2\Big(n, \frac{n}{2}, \frac{n}{2}; \frac{n+2}{2}, \frac{n+2}{2}; -e^{-2x}\Big) \\ &+ \frac{k(k-1)x^{k-2}}{n^3}\,{}_4F_3\Big(n, \frac{n}{2}, \frac{n}{2}; \frac{n+2}{2}, \frac{n+2}{2}; -e^{-2x}\Big) + \ldots + \\ &\frac{k!}{n^{k+1}}\,{}_{k+2}F_{k+1}\Big(n, (k+1)\{\frac{n}{2}\}; (k+1)\{\frac{n+2}{2}\}; -e^{-2x}\Big)\Big] + C \end{aligned} \tag{18}$$

4. FCC Violation Ratio

The UWB technology was introduced as a technique to make better use of the RF spectrum without interfering with current RF services. UWB signals are short-range, carrier-less signals that can support very high bit rates.

As aforementioned, the FCC mask regulates the UWB technology with certain EIRP regulations over the 12GHz spectrum. However, generating UWB signals that perfectly follow the FCC mask is not feasible. Therefore, the FCC VR is introduced to quantify the violation of the generated pulses to the FCC constraints. It is defined as the average power of the pulse violating the FCC mask relative to the total average power of the FCC mask. FCC VR can be used as a design parameter to help achieve the highest possible

Table 1
Results for $\int_{-\infty}^{\infty} \mathrm{sech}(x)^{2k+2} x^n \mathrm{d}x$

	x^0	x^2
$\mathrm{sech}(x)^2$	2	1.65
$\mathrm{sech}(x)^4$	1.33	0.43
$\mathrm{sech}(x)^6$	1.07	0.21
$\mathrm{sech}(x)^8$	0.91	0.13
$\mathrm{sech}(x)^{10}$	0.81	0.09
$\mathrm{sech}(x)^{12}$	0.73	0.07
$\mathrm{sech}(x)^{14}$	0.68	0.05
$\mathrm{sech}(x)^{16}$	0.64	0.04

EIRP over the widest possible band while obeying the FCC regulations.

In this work, FCC VR is mathematically defined by first defining the row vector; which is a binary vector where the ones indicate the violation of the FCC mask as shown in the following equation, and in Fig. 2:

$$\rho = \int_{\omega_1}^{\omega_2} \frac{\mathrm{sign}(X_{\mathrm{norm}}(\omega) - S_{\mathrm{FCC}}(\omega)) + 1}{4\pi \mathrm{BW}} d\omega \tag{19}$$

Where, X_{norm} from (19) is the spectrum of the generated pulse normalized to the FCC mask spectral-limit.

As illustrated in Fig. 2, the shaded area is the area that violates the FCC mask, and it is represented by the one in the binary row vector. Thus, the FCC VR is mathematically defined as follows:

$$\mathrm{FCCVR} = \frac{\int_{\Omega} \rho(\omega) \times X_{\mathrm{norm}}(\omega) d\omega}{\int_{\Omega} S_{\mathrm{FCC}}(\omega) d\omega} \tag{20}$$

Equation (20) indicates the compliance of the generated pulse to the FCC mask. Furthermore, Figs. 3 and 4 illustrate the change of

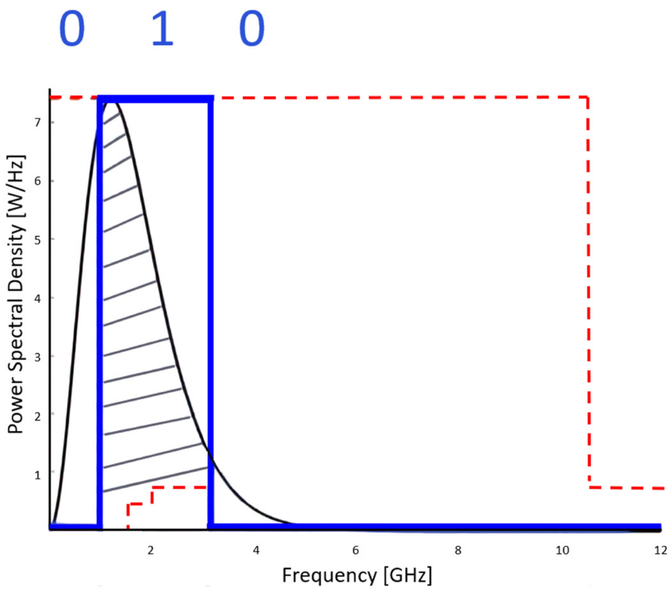

Fig. 2. Row vector for the first derivative of the Gaussian pulse.

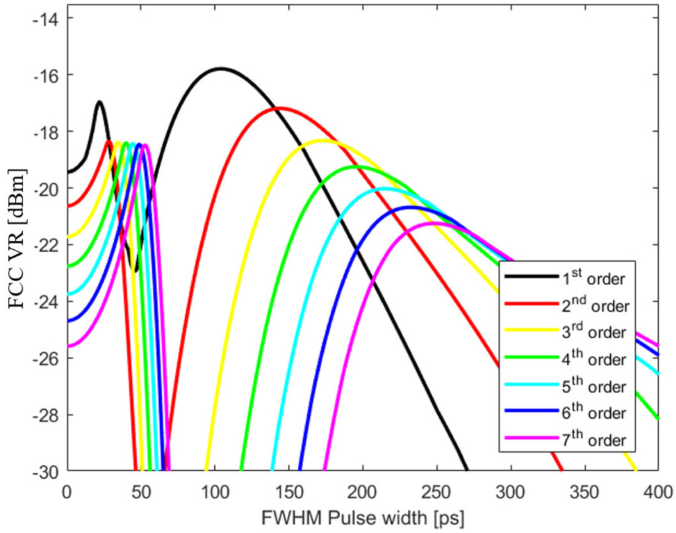

Fig. 3. FCC violation ratio varying for the seven derivatives of Gaussian function with different values for FWHM.

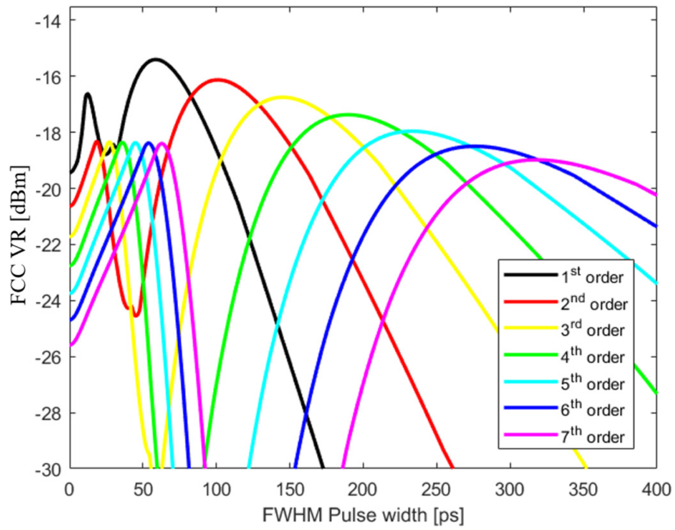

Fig. 4. FCC Violation ratio varying for the seven derivatives of Sech function with different values for FWHM.

the FCC VR with the full-width at half maximum (FWHM) for the first seven derivatives of the Gaussian and hyperbolic secant pulses respectively. As illustrated in Figs. 3 and 4, higher-order derivatives of the Gaussian- and Sech-shaped pulses reach lower FCC VR over a wider range of the FWHM.

5. The optical communications system

In this section, analysis of the basic optical communications system Fig. 1 is carried out. Furthermore, the TBP and FCC VR are applied throughout the system and proven to be very useful design parameters for a similar system.

Calculating the TBP plays two important roles in this system; it indicates the effect of the modulation on the transmitted pulse being close to its transform limit, also it provides the limitation on the design of the optical fiber as will be seen in the following section.

This work is mainly concerned with studying the communication channel (optical fiber) of the optical system Fig. 1, and applying the discussed design metrics, namely: TBP and FCC VR.

5.1. The optical fiber

Optical fibers have become a core technology in long-distance telecommunications and LANs, allowing extremely fast and low-

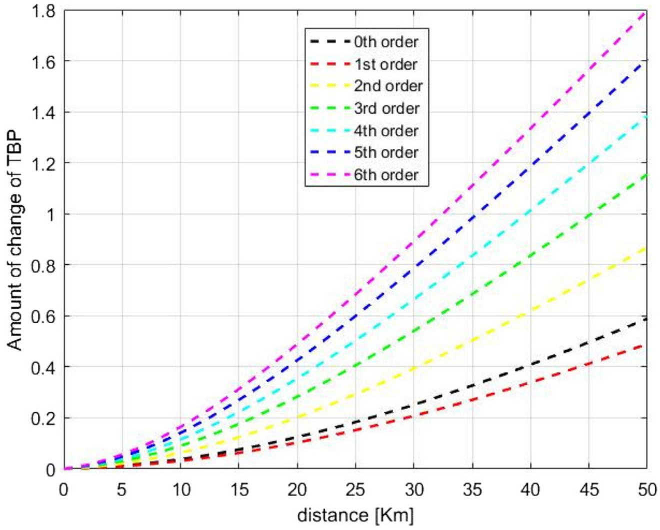

Fig. 5. Amount of change in TBP vs distance for Gaussian pulse derivatives.

cost transmission of mostly digital data. In this work, the communication channel under analysis is a single mode optical fiber (SMF).

The propagation in the SMF is characterized by the wave equation, which is then transformed to the generalized nonlinear Schrödinger equation (GNLSE) [6]. The GNLSE can be numerically solved using the split-step Fourier method (SSFM) [7], which is a pseudo spectral numerical method that is usually applied to solve nonlinear partial differential equations. This method was proven to be very accurate compared to other numerical methods [8].

5.1.1. The Time-bandwidth product

As aforementioned, TBP is a very important metric to take into consideration when designing the optical fiber. However, another critical metric emerges as well, namely the distance-bandwidth product (DBWP). The TBP and the DBWP together make a crucial design parameter relating the temporal width, spectral width, and the length of the fiber.

The DBWP is simply the product of the fiber length and the input signal bandwidth, it is a characteristic of the fiber. The TBP and the DBWP show some of the trade-offs that are present in this design problem such as, for a given data rate, there are some constraints on the bandwidth, and the temporal-width of the input pulse, also the length of the fiber. Moreover, these constraints when violated produce performance degradation such as inter-symbol interference and high bit error rate.

The TBP was calculated along the distance of the fiber for the first seven derivatives of the Gaussian pulse. Fig. 5 illustrates the amount of change that the TBP of the pulse undergoes during propagation. It is assumed that the transmitted pulses are transform-limited pulses, having the minimum TBP for the given pulse. It is worth mentioning that transform-limited pulses can minimize the effect of chromatic dispersion during propagation in the fiber. Thus, maximizing the possible transmission distance. It can be deduced from Fig. 5 that the 1^{st}-order derivative of the Gaussian pulse maintains the best performance along the fiber regarding its TBP, this observation results in a design trade-off as discussed in the following sub-section.

5.1.2. FCC Violation ratio

FCC VR was also calculated along the distance of the fiber for the first seven derivatives of the Gaussian pulse. As shown in Fig. 6, the seven derivatives of the Gaussian pulse having near-constant FCC VR along the transmission distance. The non-linearity in the SMF is the cause for the slight change in the FCC VR along propagation distance. It can be also noted, as shown in Fig. 6, that the 6^{th}- and the 4^{th}-order derivatives of the Gaussian pulse have the best FCC VR along the channel length, while the 1^{st}-order derivative has the worst FCC VR.

Fig. 5 and 6 illustrate the evident trade-off between the quality of the transmitted UWB pulse, and its compliance to the FCC constraints. It can be noted that the 2^{nd}-order derivative of the Gaussian pulse maintains great performance regarding both metrics, TBP and the FCC VR.

6. Conclusion

UWB technology has various design trade-offs and parameters; the most important is obeying the FCC regulations and constraints while maintaining the quality of the transmitted pulses. The analysis carried out, in this paper, for a complete optical communications system has proven the significance of the TBP and the FCC VR in the design process of a similar system, the TBP quantifies the quality of the signal throughout the system by measuring distortion in the pulse shape, whilst the FCC VR measures the compliance of the pulses to the FCC constraints. The mathematical closed form obtained for the TBP provides an accurate representation of the quality of UWB pulses in a similar system. The analysis provided in this paper gives great insight regarding the present trade-offs in the

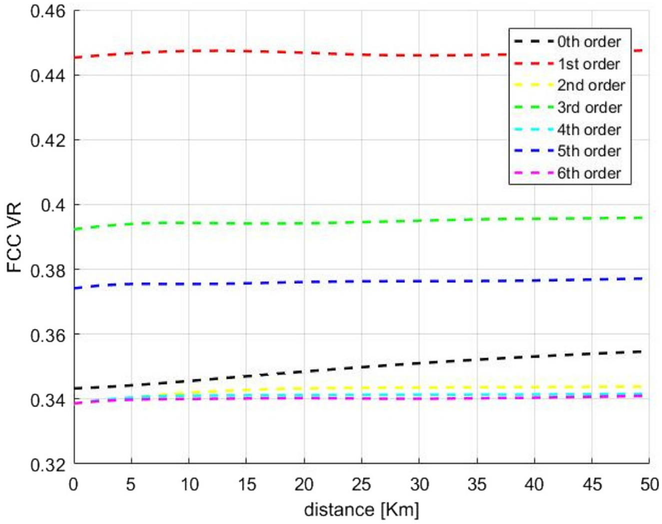

Fig. 6. FCC Violation Ratio vs Distance for Gaussian pulse derivatives of different orders.

design of the generated UWB pulses, and it was shown that the 2^{nd}-order derivative of the Gaussian pulse maintains great performance. Moreover, this mathematical analysis carried out for the first seven derivatives of the Gaussian and sech-shaped pulses is suitable for analytical synthesis and tracing of some optical devices such as the optical differentiator [9].

Acknowledgements

This work was supported by the Egyptian National Telecom Regulatory Authority (NTRA) Program CFP # 04.

References

[1] Ridwany I. Iskandar, Forecast of spectrum requirement for mobile broadband. In 2018 12th International Conference on Telecommunication Systems, Services, and Applications (TSSA) (2018 Oct) 1–5.
[2] J. Huschke, J. Sachs, K. Balachandran, J. Karlsson, Spectrum requirements for tv broadcast services using cellular transmitters. In 2011 IEEE International Symposium on Dynamic Spectrum Access Networks (DySPAN) (2011 May) 22–31.
[3] Mohamed Shehata, Mohamed Sameh Said, Hassan Mostafa, Photodetected power maximization of photonically generated impulse radio ultrawide band signals, 2018 IEEE International Symposium on Circuits and Systems (ISCAS), 05 (2018).
[4] Khristo N. Boyadzhiev, A note on bernoulli polynomials and solitons, Journal of Nonlinear Mathematical Physics (2007).
[5] Bruce R. Integrals of the form $x^k sech(x)^n$. http://www.ramapodesign.com/bruce/math/math.php?f=xnSechx.html, 2007.
[6] Govind Agrawal, Chapter 3 - group-velocity dispersion, in: Govind Agrawal (Ed.), Nonlinear Fiber Optics (Fifth Edition), Optics and Photonics, fifth edition edition, Academic Press, Boston, 2013, pp. 57–85.
[7] Jong-hyung Lee, Analysis and Characterization of Fiber Nonlinearities with Deterministic and Stochastic Signal Sources, PhD thesis, 01, (2000).
[8] Pablo Suarez, An introduction to the split step fourier method using matlab. 09, (2015).
[9] Mohammad H. Asghari, José Azaña, Proposal and analysis of a reconfigurable pulse shaping technique based on multi-arm optical differentiators, Optics Communications 281 (18) (2008) 4581–4588.